Title

Water-Soluble 3D Covalent Organic Framework that Displays an Enhanced Enrichment Effect of Photosensitizers and Catalysts for the Reduction of Protons to H2

Journal

ACS Applied Materials & Interfaces, 12(1)

ISSN

1944-8244

Authors

Gao, Zhong-Zheng

Wang, Ze-Kun

Wei, Lei

et al.

Publication Date

2020-01-08

DOI

10.1021/acsami.9b19870

Peer reviewed

ACS APPLIED MATERIALS & INTERFACES

Functional Nanostructured Materials (including low-D carbon)

A Water-Soluble 3D Covalent Organic Framework That Displays Enhanced Enrichment Effect of Photosensitizers and Catalysts for the Reduction of Protons to H2

Zhong-Zheng Gao, Ze-Kun Wang, Lei Wei, Guangqiang Yin, Jia Tian, Chuanzhi Liu, Hui Wang, Dan-Wei Zhang, Yue-Biao Zhang, Xiaopeng Li, Yi Liu, and Zhan-Ting Li

ACS Appl. Mater. Interfaces, **Just Accepted Manuscript** • Publication Date (Web): 02 Dec 2019

Just Accepted

is published by the American Chemical Society. 1155 Sixteenth Street N.W., Washington, DC 20036

A Water-Soluble 3D Covalent Organic Framework That Displays Enhanced Enrichment Effect of Photosensitizers and Catalysts for the Reduction of Protons to H_2

Zhong-Zheng Gao,[†] Ze-Kun Wang,[†] Lei Wei,[‡] Guangqiang Yin,[§] Jia Tian,[†] Chuan-Zhi Liu,[†] Hui Wang,[†] Dan-Wei Zhang,[†] Yue-Biao Zhang,[‡] Xiaopeng Li,[§] Yi Liu,*[,¶] and Zhan-Ting Li*[,†]

[†]Department of Chemistry, Shanghai Key Laboratory of Molecular Catalysis and Innovative Materials, Fudan University, 2205 Songhu Road, Shanghai 200438, China

[‡]School of Physical Science and Technology, ShanghaiTech University, Shanghai 201210, China

[§]Department of Chemistry, University of South Florida, Tampa, Florida 33620, USA

[¶]The Molecular Foundry, Lawrence Berkeley National Laboratory, One Cyclotron Road, Berkeley, California 94720, USA

KEYWORDS: covalent organic framework, supramolecular organic framework, three-dimensional polymer, visible light photocatalysis, hydrogen generation

ABSTRACT: Covalent organic frameworks (COFs) are emerging porous polymers that have 2D or 3D long-range ordering. Currently available COFs are typically insoluble or decompose upon dissolution, which remarkably restricts their practical implementations. For 3D COFs, the

achievement of non-interpenetration, which maximizes their porosity-derived applications, also remains a challenge synthetically. Here we report the synthesis of the first highly water-soluble 3D COF (sCOF-101) from irreversible polymerization of a preorganized supramolecular organic framework through cucurbit[8]uril (CB[8])-controlled [2 + 2] photodimerization. Synchrotron X-ray scattering and diffraction analyses confirm that sCOF-101 exhibits porosity periodicity, with a channel diameter of 2.3 nm, in both water and the solid state and retains the periodicity under both strongly acidic and basic conditions. As an ordered 3D polymer, sCOF-101 can enrich $[Ru(bpy)_3]^{2+}$ photosensitizers and redox-active polyoxometalates in water, which leads to remarkable increase of their photocatalytic activity for proton reduction to produce H_2.

INTRODUCTION

The physical and chemical properties of COFs are, to a considerable extent, dictated by the nature of the covalent linkages.[1–15] In most cases, reversible bonds, such as boroxine,[1] imine,[16–20] or hydrazine,[21] are used as linkages to achieve regularity. Nevertheless, the resulting structures frequently suffer instability in aqueous media, which has been one of three key issues needed to be resolved for any practical/industrial applications of COFs.[15] Thus, in recent years, less reversible or irreversible bonds, including triazine,[22–24] phenazine,[25] dioxin,[26,27] imide,[28] or olefin,[29–32] have been explored for the generation of COFs with increased stability. Examples of irreversible covalent "locking" of dynamic frameworks by forming oxazole and thiazole have also been reported.[33–35] However, all the reported structures maintain their frameworks only in the solid state, and examples of water-stable structures are very scarce.[23,24,36] We envisioned that COFs that are soluble in water, the best environmentally benign solvent, might help to realize increased processability and scalability,[37] another two key issues that are needed to address for practical

applications.[15] To the best of our knowledge, strategies for the generation of water-soluble COFs have not been available.

Taking the above considerations in mind, we herein report the synthesis of the first water-soluble 3D covalent organic framework, termed sCOF-101, by utilizing a periodic supramolecular organic framework as template to direct the [2 + 2] photodimerization of the styrylpyridinium units. We demonstrate that sCOF-101, as a new 3D ordered polymer, is highly stable in harsh acidic and basic media, does not suffer from interpenetration, which substantially decreases the pore size of 3D COFs but can be rarely avoided,[38] and is able to enrich Ru^{2+}-complex photosensitizers and redox-active polyoxometalates, which leads to significant increase of their photocatalytic activity, as compared with an irregular polymer counterpart.

EXPERIMENTAL SECTION

General methods. All reagents were obtained from commercial suppliers and used without further purification unless otherwise noted. All reactions were carried out under a dry nitrogen atmosphere. All solvents were dried before use following standard procedures. ^{1}H and ^{13}C NMR spectra were recorded on 400 MHz spectrometers in the indicated solvents at room temperature (298 K). Solid-state or solution-phase synchrotron X-ray scattering experiments were performed on the BL16B1 beamline of Shanghai Synchrotron Radiation Facility (SSRF), using a fixed wavelength of 0.124 nm, a sample-to-detector distance of 1.85m and an exposure time of 2000 s. The 2D scattering pattern was collected on a charge coupled device camera, and the curve intensities versus q were obtained by integrating the data from the pattern. Solid-state synchrotron X-ray diffraction experiments were performed at beamline BL14B1 of the Shanghai Synchrotron Radiation Facility (SSRF) at a wavelength of 0.688 Å. BL14B1 is a beamline based on bending magnet and a Si (111) double-crystal monochromator was used to monochromatize the beam. The

size of the focus spot is about 0.5 mm and the end station is equipped with a Huber 5021 diffractometer. NaI scintillation detector was used for data collection. Scanning electron micrographs of the samples were obtained on a Nova nano SEM 450 Field Emission Scanning Electron Microscope at 3.00 kV with the material adhered to the SEM sample holder directly or on a Phenom Scanning Electron Microscope at 15.00 kV after the material that adhered to the sample holder was been gilded to 10^{-1}-10^{-2} vacuum degree. Transmission electron micrographs were recorded on a JEM 2011 FETEM microscope at 200 kV aligned for low dose (10 e $Å^{-2}$ s^{-1}) diffractive imaging. Dynamic light scattering (DLS) measurement were conducted on a Malvern Zetasizer Nano ZS90 using a monochromatic coherent He–Ne laser (633 nm) as the light source and a detector that detected the scattered light at an angle of 90°. Thermogravimetric analysis (TGA) experiments were performed on a Model TGA/SDTA 851 instrument. Samples were placed in alumina pans and heated at a rate of 5 °C per minute from 30 to 800 °C under a nitrogen atmosphere. Isothermal titration calorimetry (ITC) experiment was carried out using a MicroCal PEAQITC instrument. Association constants and associated thermodynamic parameters were obtained through computer simulations (curve fitting) using MicroCal ITC analyze software. UV-Vis spectra were detected on a Perkin-Elmer 750s instrument from 200-800 nm at the scan rate of 3 nm/internal. Fluorescence measurements were performed on a VARIAN CARY Eclipse Fluorescence Spectrophotometer and PerkinElmer LS 55 Luminescence spectrometer. The EtOH vapor adsorption isotherms were collected using MicrotracBELSopr-Aqua3 adsorption apparatus with a water circulator bath. Anhydrous EtOH was used for vapor adsorption, which degassed at least five times before isotherm collection. The crystal data for complex $(\mathbf{M1})_2$⊂CB[8] has been deposited at The Cambridge Crystallographic Data Centre (CCDC) (no. 1951214).

The synthesis of sCOF-101. A solution of SOF-s (0.20 g) in water (10 mL) was stirred and subjected to a 300-W solid state light source. The solution was kept at 25 °C using a powerful fan. After 4 hours, SOF-s was converted into sCOF-101 completely, which was confirmed by 1H NMR for a sample of SOF-s of the same concentration in D_2O.

The synthesis of P-irr. This polymer was prepared from **T1** by using the procedures described above for sCOF-101.

Photochemical reactivity studies. Photoirradiation was carried-out with a 300 W solid state light source. Prior to irradiation, the samples were degassed with N_2 gas for 30 min. The samples were kept under magnetic stirring during the irradiation process. The solution was kept at 25 °C using a powerful fan.

The H_2 production reactions in the aqueous solution. The reaction was carried out in an external illumination-type reaction vessel with a magnetic stirrer. Samples were prepared in 10 mL septum-sealed glass vials. Each sample was made up to a volume of 2.0 mL of methanol (20%, v/v) aqueous solution with the pH value of 1.8 (adjusted by adding 2 M HCl). Sample vials were capped and deoxygenated by bubbling nitrogen through them for 30 min to ensure complete air removal. The solution was irradiated by a 300 W solid state light source. The H_2 gas formed in the headspace of the vial was analyzed by GC.

RESULTS AND DISCUSSION

The [2 + 2] photodimerization of 1,2-disubstitued ethylenes is robust for the synthesis of polymers,[39] which can be further accelerated by cucurbit[8]uril (CB[8]) encapsulation.[40–44] We prepared compound **M1** (Figure 1) to study its binding with CB[8]. The X-ray crystal structure analysis revealed that CB[8] encapsulates two molecules of **M1** (Figure 1), with the two 4-vinylpyridinium (VP) units stacking in an *anti*-parallel manner in its cavity. This anti-parallel 2:1

binding motif is ideal for the construction of 3D networks from multitopic building blocks.[45–47] We then prepared highly water-soluble tetrahedral molecule **T1** (Figure 1) and studied its co-assembly with CB[8] for the formation of a new reactive 3D SOF. The 1:2 mixture of **T1** and CB[8] in water maintained homogeneity at [**T1**] = ≥ 4.0 mM.

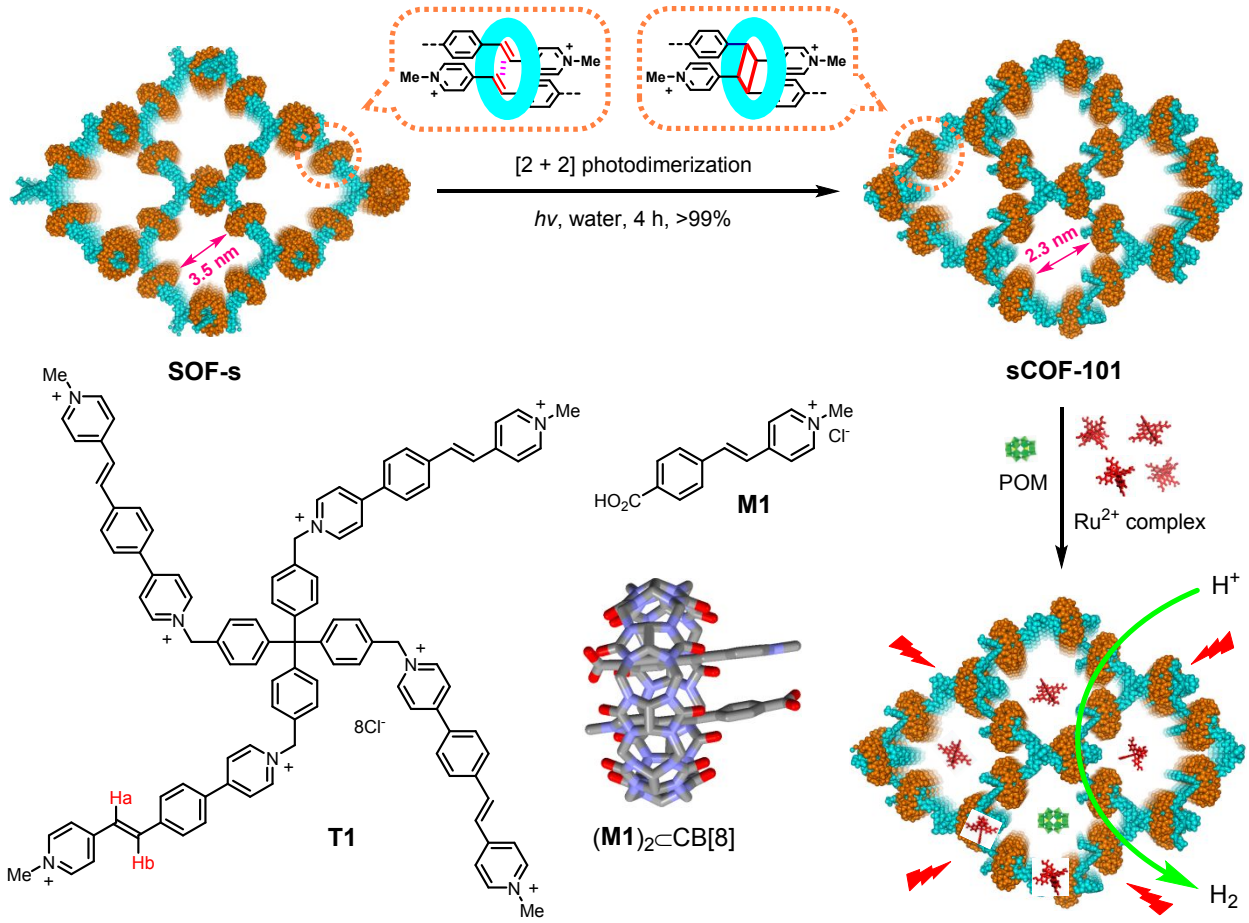

Figure 1. Monomers **T1** and **M1**, the crystal structure of complex (**M1**)$_2$⊂CB[8] (CCDC no. 1951214) and schematic representation of supramolecular organic framework SOF-s, water-soluble covalent organic framework sCOF-101 and its promotion of visible light-induced reduction of protons into H_2 through enrichment of POM catalysts and Ru^{2+}-complex photosensitizers.

Our previous work had established the co-assembly of a prototype tetrahedral monomer and CB[8] into a water-soluble periodic supramolecular organic framework (SOF).[48] We envisioned

that the co-assembly of **T1** and CB[8] should give rise to a similar system, which we characterized using the established methods.[48] In brief, ^{1}H NMR titration experiments in D_2O indicated that the ethylene units of **T1** were encapsulated in the cavity of CB[8] (Figures S1 and S2), while fluorescence and absorption experiments supported their 1:2 stoichiometry and the 2:1 binding pattern between the styryl units of **T1** and CB[8] (Figures S3–S5). The apparent association constant (K_a) of their 2:1 complex was determined by the isothermal calorimetric titrations (Figure S6) to be 7.7 (± 0.8) × 10^{12} M^{-2}. The related ΔH and $-T\Delta S$ were −7.9 (± 0.25) and −5.2 kcal/mol, respectively, which indicates that the binding was both enthalpy and entropy-driven. The K_a was substantially larger than that (1.1 (± 0.047) × 10^{11} M^{-2}) of the 2:1 complex formed by **M1** and CB[8] (Figure S6), which reflects the multivalence of the binding of **T1** with CB[8].[49,50] Dynamic light scattering (DLS) experiments for the 1:2 solution of **T1** and CB[8] in water revealed the formation of nano-scaled assemblies (Figure S7). At [**T1**] = 4.0 mM, the hydrodynamic diameter (D_H) was determined to be 220 nm. The D_H value decreased with the dilution of the solution. However, even at [**T1**] = 15 μM, D_H was still as high as 14 nm. In contrast, at 4.0 mM, **T1** formed much smaller entities (D_H = 6.5 nm) (Figure 2a) due to intermolecular stacking. All these observations supported that, similar to the reported prototype,[48] styrene-derived **T1** and CB[8] co-assembled in water into a new 3D supramolecular organic framework (SOF-s, Figure 1).

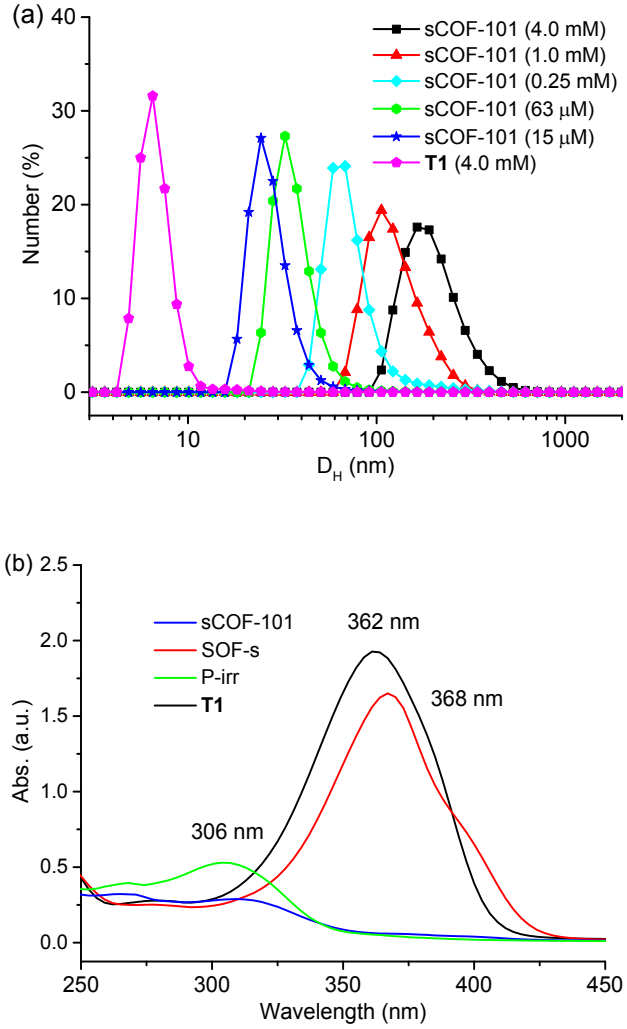

Figure 2. (a) DLS profile of sCOF-101 and **T1** in water at 25 °C. The concentration indicated for sCOF-101 represents that of **T1** of SOF-s for the preparation of the polymers. (b) The UV−vis absorption spectrum of sCOF-101, SOF-s, P-irr and **T1** in water at 25 °C ([**T1**] = 10 μM).

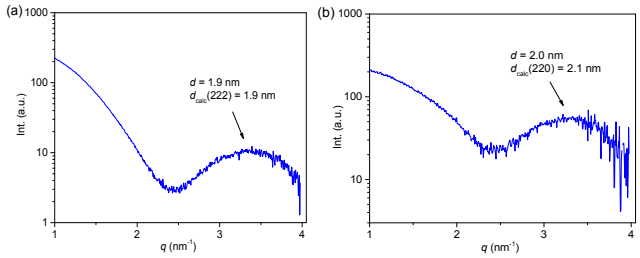

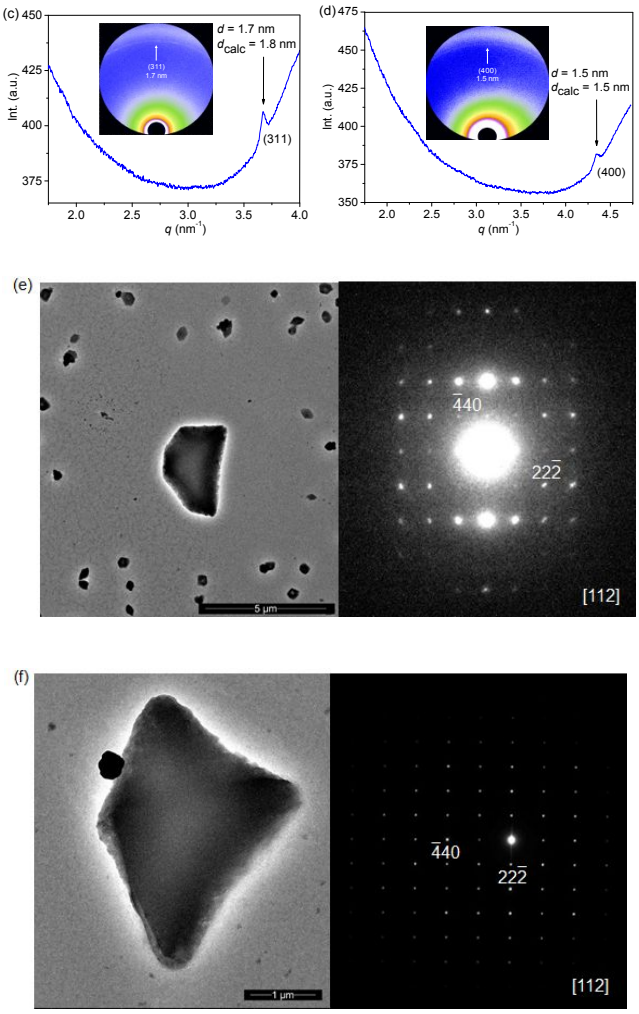

Figure 3. (a,b) Solution-phase SAXS profile of SOF-s and sCOF-101 ([**T1**] = 4.0 mM) in water. (c,d) SAXS profile of SOF-s and sCOF-101 microcrystals (inset: 2D profile). (e,f) TEM images of sCOF-101 and SOF-s microcrystal with the SAED pattern.

The synchrotron small-angle X-ray scattering (SAXS) profile of SOF-s ([**T1**] = 4.0 mM) in water gave rise to a broad, but conspicuous peak centred around 1.9 nm (Figure 3a). The *d*-spacing can be assigned to the {222} of the SOF-s model. The broadness of the peak reasonably reflected the dynamic nature of the self-assembled framework in solution. Slow evaporation of the above solution at room temperature produced microcrystals. Synchrotron SAXS profile of the microcrystals displayed one sharp peak centered at 1.8 nm (Figure 3c), which was also reflected

on the 2D profile (Figure 3c, inset). This peak matched with the calculated {311} spacing (1.7 nm). All the experiments, joining together, provided consistent evidences to support that SOF-s possessed periodicity in both solution and solid states. Thermogravimetric analysis showed that SOF-s was stable up to 360 °C (Figure S8). The weight loss of ~8% under 100 °C might be ascribed to the evaporation of adsorbed water.

^{1}H NMR spectra in D_2O showed that SOF-s was stable at room temperature. However, upon visible light irradiation, the ethylene units of the **T1** molecules readily underwent [2 + 2] photodimerization to afford new water-soluble covalent organic framework sCOF-101 (Figure 1). The photodimerization was completed after about 4 hours, as indicated by ^{1}H NMR spectrum, which revealed the vanishing of their diagnostic H-a and H-b signals (Figures 1 and S9). UV−vis absorption experiments further confirmed this photodimerization process. Upon irradiation, the absorption band of the styrene-incorporated conjugated aromatic arms, which centered around 368 nm, weakened quickly during the first ten minutes, then further decreased slowly, and finally vanished after about 8 hours (Figures 2 and S10). Accompanied with the weakening of this absorption band, an absorption band centered at 308 nm was generated, which could be assigned to the 4-phenylpyridinium units, the remaining largest conjugated moieties of the resulting sCOF-101. By comparing the absorbance at 368 nm before and after the irradiation, we could determine the yield of the photodimerization to be >99%. Irradiation also caused the emission of sCOF-101 around 500 nm to disappear completely and the resulting sCOF-101 gave rise to a strong emission around 450 nm (Figure S11). sCOF-101 was soluble in water at the studied highest concentration ([**T1**] = 4.0 mM). DLS revealed that sCOF-101 obtained from the SOF-s solution at [**T1**] = 4.0 mM had a D_H of 165 nm, which was notably smaller than that (220 nm) of the corresponding precursor SOF-s of the identical concentration. This reduction might partially reflect the contracted

aperture (2.3 nm) of sCOF-101 as compared with that of the SOF-s (3.5 nm) (Figure 1). The D_H value of sCOF-101 decreased with the decrease of the concentration (Figures 2 and S12), indicating that the larger polymeric particles were formed through the aggregation of smaller ones.

Synchrotron SAXS profile of the solution of sCOF-101 ([**T1**] = 4.0 mM) in water gave rise to a broad, but discernible peak centered around 2.0 nm (Figure 3b), which matched with the {113} spacing (2.1 nm) obtained for the modelled structure. Slow evaporation of the above solution afforded microcrystals of sCOF-101. Their synchrotron SAXS profile gave one sharp peak centered at 1.5 nm (Figure 3d), which was also displayed on the 2D profile (Figure 3d, inset). This peak matched with the calculated spacing (1.5 nm) of the {400} spacing of the modelled structure. The synchrotron XRD profile of the microcrystals exhibited two broad, but distinguishable peaks around 0.8 and 1.5 nm (Figure S13), respectively, which could be assigned to the {262} and {400} spacings of the modelled structure. All these results supported that sCOF-101 possessed regularity or periodicity in aqueous solution as well as in the solid state. Thermogravimetric analysis showed that the stability of sCOF-101 was comparable to that of SOF-s (Figure S8). The formation of microcrystals by sCOF-101 and SOF-s was also confirmed by transmission electron microscope (TEM) with the selected area electron diffraction (SAED) (Figures 3e and 3f), which showed their electron diffraction patterns both in the 112 zone. The SAED pattern of sCOF-101 showed the {–440} and {22–2} lattice spacings (1.0 nm and 1.3 nm), whereas that of SOF-s pointed to the {–440} lattice spacing (1.4 nm) and the {222} lattice spacing (2.0 nm). The results further supported the crystallinity and regularity of the new COF, which was realized through the direction of SOF-s. High-resolution TEM image also exhibited lattice fringes for the selected particle (Figure S14). The fringe spacing is about 2.1 Å, fitting the modelled {220} spacing. Elemental

mapping analysis for the microcrystals of SOF-s and sCOF-101 also confirmed the compositions of the C, N, O and Cl elements (Figures S15 and S16).

To reveal the role of CB[8] for the formation of the regularity of sCOF-101, we further investigated the [2 + 2] photodimerization of **T1** in water. Upon visible light irradiation, **T1** also underwent the photodimerization reaction to afford irregular porous polymer P-irr. Irradiating the solution for 4 hours caused the absorption band, centered at 362 nm, of the peripheral styrene-incorporated conjugated units of **T1** to disappear completely (Figures 2 and S17), which indicated that the photodimerization took place quantitatively. Moreover, at [**T1**] = 4.0 mM, no precipitate was observed after the photodimerization. DLS experiment for the solution of the resulting P-irr ([**T1**] = 4.0 mM) in water afforded a D_H value of 164 nm (Figure S18). The D_H also became smaller with the dilution of the solution, which again indicated that the larger particles were generated via the aggregation of smaller polymeric particles. Thermogravimetric analysis showed that the polymer was stable up to 280 °C (Figure S19). As expected, no peaks were observed in the SAXS or XRD profile of P-irr in solution or the solid state, reflecting the irregularity of its polymeric backbone. DLS experiments also revealed that sCOF-101 maintained its framework in harsh acidic (HCl, 3 M) or basic (NaOH, 1 M) solution (Figure S20). In contrast, in the identical acidic or basic solution, P-irr turned into insoluble, dark solids, which supported that CB[8] stabilized the encapsulated cyclobutene units of sCOF-101. However, ^{1}H NMR spectrum showed that hearting the solution of both samples in D_2O at 95 °C for 10 hours did not cause the occurring of the peaks of the –C*H*=C*H*– unit, indicating that both samples were stable at high temperature.

Vapor adsorption isotherms of ethanol and water were collected on sCOF-101, SOF-s and P-irr at 283 K (Figures 4a and 4b). Although the uptake patterns were a little different, all the three polymers displayed high adsorption ability for either of the solvents, as observed for reported

crystalline covalent organic frameworks.[51,52] The pore volume calculated from the uptake of the two solvents was very close, supporting that the backbones of the polymer maintained the rigidity with no important deformation. In contrast, both SOF-s and P-irr gave rise to different values with the two solvents. For SOF-s, this difference may be rationalized by considering different levels of the sliding of the styrylpyridinium units encapsulated in the CB[8] cavity upon solvent uptake. For P-irr, we tentatively attributed the difference to different levels of deformation of the backbones caused by solvent uptake.

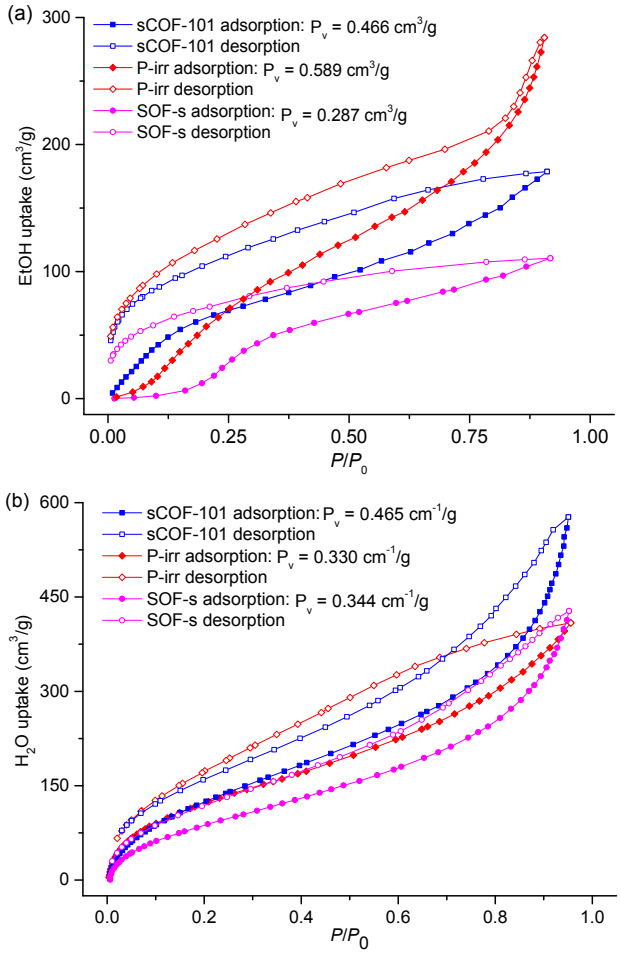

Figure 4. (a) EtOH and (b) water vapor adsorption isotherms of sCOF-101, SOF-s and P-irr at 283 K.

Structural modelling revealed that sCOF-101 and SOF-s had a 3D framework that resembles that of the diamond net. Their void volumes were calculated to be 88% and 90%, respectively,

whereas the apertures, defined by the six CB[8] rings that produced a cyclohexane-like chair conformation, was calculated to be 2.3 and 3.5 nm (Figure 2), respectively. Fluorescence quenching experiments indicated that both sCOF-101 and SOF-s adsorbed ruthenium-complex photosensitizers $(Ru(BDC)_3]^{4-}$, as K^+ salt, BDC = 2,2'-bipyridyl-5,5'-dicarboxylate) and $Ru(BPY)_2(BDC)$, BPY = 2,2'-bipyridine) and redox-active POM catalysts (Wells–Dawson-type $[K_6P_2W_{18}O_{62}]$ (WD-POM) and Keggin-type $Na_3PW_{12}O_{40}$ (K1-POM) and $K_4W_{12}SiO_4O_{36}$ (K2-POM)) in water (Figures S21–S26). DLS experiments in water showed that both frameworks maintained the nano-scaled structures after guest uptake (Figures S27– S29).

The capacity of sCOF-101 and P-irr in improving the photocatalytic efficiency of the Ru^{2+}-POM systems for the reduction of protons to H_2 was then investigated using conditions established for a fully rigid SOF.[53-55] Compared with that of the control solution that contained neither of the polymers, the turnover number (TON), defined as $n(1/2H_2)/n(POM)$, of the solution containing sCOF-101 and P-irr, obtained for six combinations of the sensitizers and catalysts, was increased by 5.9-8.8 and 2.0-2.8-fold, respectively (Figure 5a), which indicated that the regularity of sCOF-101 significantly promoted the catalyzing ability of the bi-component catalytic systems.

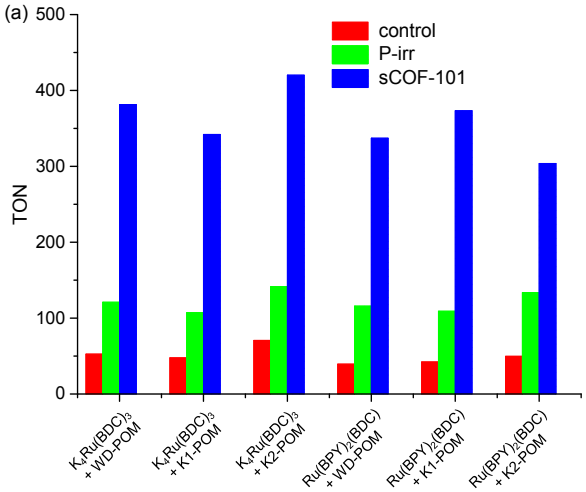

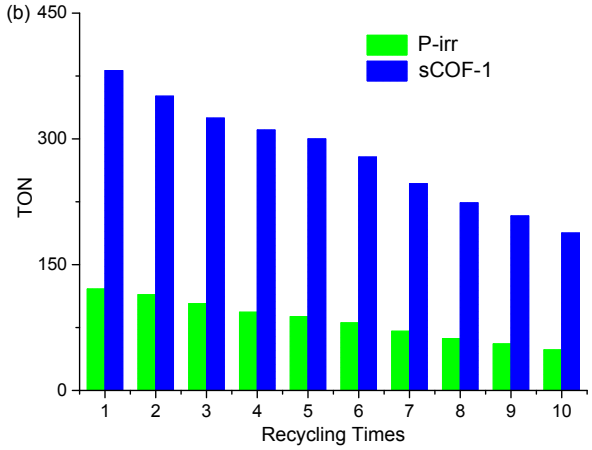

Figure 5. a) TON values in H_2O and MeOH (4:1, v/v, pH = 1.8/HCl) containing different photosensitizer (20 μM) and POM catalyst (2.0 μM) in the absence (control) or presence of sCOF-101 or P-irr ([**T1**] = 0.1 mM). b) TON versus recycling times for the $K_4Ru(BDC)_3$/K1-POM system in the solution of sCOF-101 or P-irr. Irradiation time: 22 h.

In the absence of the ruthenium complexes, no H_2 production was observed in the solution of sCOF-101 or P-irr. Under the conditions used for the system of sCOF-101, SOF-s of the identical concentration also promoted the production of H_2. However, the promotion was generally lower than that of sCOF-101 (Figure S30), even though the irradiation would lead to partial conversion of SOF-s to sCOF-101. Compared with that of a previously reported SOF assembled from a fully rigid tetrahedral component,[54] TON realized by SOF-s was comparable.

For all the catalytic systems, H_2 evolution could last for a long time. For the combination of $[Ru(BDC)_3]^{4-}$ and WD-POM, the time was about 60 hours. Further elongating the irradiation could not lead to observable amount of H_2. However, after being left to stand for about 12 hours, without adding new polymer, photosensitizer or POM catalyst, irradiating the solution could bring about the generation of H_2 again. After repeating for 10 times, the system could still exhibit a considerable catalytic activity. The results for the $K_4Ru(BDC)_3$/K1-POM system are provided in

Figure 5b. DLS profile of the solution after repeated use for 10 times afforded a D_H of 64 nm, which was comparable to that (65 nm) of the originally prepared solution, indicating that sCOF-101 was very stable and could survive after repeated irradiation. P-irr-mediated catalytic system could also be used repeatedly. Nevertheless, its catalytic activity was consistently lower by 3.1-4.0 times than that of sCOF-101, which again reflected the importance of the regularity of sCOF-101 in improving the catalytic activity. In the absence of either of the polymers, irradiating the solution also resulted in the evolution of H_2, which could last about 45 hours. However, after standing overnight, further irradiating the solution could not cause the evolution of H_2. These results appeared to indicate that the inclusion of the photosensitizer and catalyst molecules into the polymer could increase their stability. UV-vis absorption spectrum showed that, after the acidic photocatalysis conditions, irradiating the solution of sCOF-101 for 5 hours did not cause observable ring opening of the [2 + 2] photodimers. Synchrotron SAXS profile of the solid sample, obtained by slow evaporation of the solution of sCOF-101 after photocatalysis, exhibited the [400] peak as observed for the original sCOF-101 example, which supported the integrity of the material.

CONCLUSIONS

In summary, by making use of the covalent locking of a new periodic supramolecular organic framework, we have realized the construction of the first water-soluble covalent organic framework that possesses periodic porosity in solution. The new ordered 3d polymer exhibits strong inclusion ability for ruthenium complex photosensitizers and redox-active polyoxometalate catalysts of very low concentration. The inclusion leads to important enrichment effect that, as compared with an irregular system, significantly enhances electron transfer from photo-initiated Ru^{2+}-complex sensitizer triplet species to the POM catalysts and consequently photocatalytic reduction of protons into hydrogen. The result represents the first step for the synthesis of regular,

rigid three-dimensional polymer frameworks using the "conventional" synthetic strategy to form non-dynamic covalent bonding. The methodology should open new opportunities for the construction of soluble 2D and 3D COFs with tunable structures and functions.

ASSOCIATED CONTENT

Supporting Information.

^{1}H and ^{13}C NMR, fluorescence and absorption spectra, ITC, DLS, TGA and vapor adsorption isotherm profiles, TEM images, and hydrogen evolution profile. This material is available free of charge via the Internet at http://pubs.acs.org.

AUTHOR INFORMATION

Corresponding Authors

* E-mail: yliu@lbl.gov

* E-mail: ztli@fudan.edu.cn

ORCID

Dan-Wei Zhang: 0000-0003-1244-1850

Yue-Biao Zhang: 0000-0002-8270-1067

Xiaopeng Li: 0000-0001-9655-9551

Yi Liu: 0000-0002-3954-6102

Zhan-Ting Li: 0000-0003-3954-0015

Notes

The authors declare no competing financial interest.

Author Contributions

Z.T.L., Y.L., C.Z.L., H.W. and D.W.Z. conceived the project. Z.Z.G., Z.K.W., L.W., G.Y., J.T., and C.Z.L. performed the experiments. Z.T.L., Y.L., C.Z.L., Y.B.Z. and X.L. analyzed the data. Z.T.L., Y.L. and Z.Z.G. co-wrote the manuscript. All authors participated in the discussion and commented on the results.

ACKNOWLEDGMENT

This work was supported by NSFC (Grant numbers: 21890732 and 21921003). We are grateful for Shanghai Synchrotron Radiation Facility for providing the beam time (beamlines BL16B1 and BL14B1). YL thanks the support from the Molecular Foundry, a national user facility supported by the Office of Science, Office of Basic Energy Sciences, of the U.S. Department of Energy under Contract No. DE-AC02-05CH11231. Solution-phase SAXS data was collected at the Advanced Light Source (ALS), SIBYLS beamline on behalf of US DOE-BER, through the Integrated Diffraction Analysis Technologies (IDAT) program. Additional support comes from the NIGMS project ALS-ENABLE (P30 GM124169) and a High-End Instrumentation Grant S10OD018483. The authors thank Prof. Qiaowei Li at Fudan University for beneficial discussions.

REFERENCES

(1) Côté, A. P.; Benin, A. I.; Ockwig, N. W.; O'Keeffe, M.; Matzger, A.J.; Yaghi, O. M. Porous, Crystalline, Covalent Organic Frameworks. *Science* **2005**, *310*, 1166−1170.

(2) Ding, S. Y; Wang, W. Covalent organic frameworks (COFs). From design to applications. *Chem. Soc. Rev.* **2013**, *42*, 548−568.

(3) Feng, X.; Ding, X.; Jiang, D. Covalent organic frameworks. *Chem. Soc. Rev.* **2012**, *41*, 6010−6022.

(4) Liu, X.-H.; Guan, C.-Z.; Wang, D.; Wan, L.-J. Graphene-like single-layered covalent organic frameworks: synthesis strategies and application prospects. *Adv. Mater.* **2014**, *26*, 6912−6920.

(5) Bisbey, R.P.; Dichtel, W. R. Covalent Organic Frameworks as a Platform for Multidimensional Polymerization. *ACS Central Sci.* **2017**, *3*, 533−543.

(6) Jin, Y.; Hu. Y.; Zhang, W. Tessellated multiporous two-dimensional covalent organic frameworks. *Nat. Rev. Chem.* **2017**, *1*, 0056.

(7) Wu, M.-X.; Yang, Y.-W. Applications of covalent organic frameworks (COFs): From gas storage and separation to drug delivery. Chin. Chem. Lett. 2017, 28, 1135-1143.

(8) Babu, H. V.; Bai, M. G. M.; Rao, R. M. Functional π-Conjugated Two-Dimensional Covalent Organic Frameworks. *ACS Appl. Mater. Interfaces* **2019**, *11*, 11029–11060.

(9) Pardakhti, M.; Jafari, T.; Tobin, Z.; Dutta, B.; Moharreri, E.; Shemshaki, N. S.; Suib, S.; Srivastava, R. Trends in Solid Adsorbent Materials Development for CO_2 Capture. *ACS Appl. Mater. Interfaces* **2019**, *11*, 34533–34559.

(10) Yuan, F.; Tan, J.; Guo, J. Assemblies of covalent organic framework microcrystals: multiple-dimensional manipulation for enhanced applications. *Sci. China Chem.* **2018**, *61*, 143−152.

(11) Dong, R.; Zhang, T.; Feng, X. Interface-Assisted Synthesis of 2D Materials: Trend and Challenges. *Chem. Rev.* **2018**, *118*, 6189−6235.

(12) Liang, R.-R.; Zhao, X. Heteropore covalent organic frameworks: a new class of porous organic polymers with well-ordered hierarchical porosities. *Org. Chem. Front.* **2018**, *5*, 3341−3356.

(13) Song, Y.; Sun, Q.; Aguila, B.; Ma, S. Opportunities of Covalent Organic Frameworks for Advanced Applications. *Adv. Sci.* **2019**, *6*, 1801410.

(14) Zheng, C.; Zhu, J.; Yang, C.; Lu, C.; Chen, Z.; Zhuang, X. The art of two-dimensional soft nanomaterials. *Sci. China Chem.* **2019**, *62*, 1145−1193.

(15) Kandambeth, S.; Dey, K.; Banerjee, R. Covalent Organic Frameworks: Chemistry beyond the Structure. *J. Am. Chem. Soc.* **2019**, *141*, 1807−1822.

(16) Uribe-Romo, F.J.; Hunt, J.R.; Furukawa, H.; Klöck, C.; O'Keeffe, M.; Yaghi, O. M. A crystalline imine-linked 3-D porous covalent organic framework. *J. Am. Chem. Soc.* **2009**, *131*, 4570−4571.

(17) Ding, S.Y.; Gao, J.; Wang, Q.; Zhang, Y.; Song, W. G.; Su, C. Y.; Wang, W. Construction of covalent organic framework for catalysis: Pd/COF-LZU1 in Suzuki-Miyaura coupling reaction. *J. Am. Chem. Soc.* **2011**, *133*, 19816−19822.

(18) Ma, T.; Kapustin, E. A.; Yin, S. X.; Liang, L.; Zhou, Z.; Niu, J.; Li, L. H.; Wang, Y.; Su, J.; Li, J.; Wang, X.; Wang, W. D.; Wang, W.; Sun, J.; Yaghi, O. M. Single-crystal x-ray diffraction structures of covalent organic frameworks. *Science* **2018**, *361*, 48–52.

(19) Segura, J. L.; Mancheno, M. J.; Zamora, F. Covalent organic frameworks based on Schiff-base chemistry: synthesis, properties and potential applications. *Chem. Soc. Rev.* **2016**, *45*, 5635−5671.

(20) Bhadra, M.; Sasmal, H. S.; Basu, A.; Midya, S. P.; Kandambeth, S.; Pachfule, P.; Balaraman, E.; Banerjee, R. Predesigned Metal-Anchored Building Block for In Situ Generation of Pd Nanoparticles in Porous Covalent Organic Framework: Application in Heterogeneous Tandem Catalysis. *ACS Appl. Mater. Interfaces* **2017**, *9*, 13785–13792.

(21) Bunck, D. N.; Dichtel, W. R. Bulk synthesis of exfoliated two-dimensional polymers using hydrazone-linked covalent organic frameworks. *J. Am. Chem. Soc.* **2013**, *135*, 14952−14955.

(22) Kuhn, P.; Antonietti, M.; Thomas, A. Porous, covalent triazine-based frameworks prepared by ionothermal synthesis. *Angew. Chem. Int. Ed.* **2008**, *47*, 3450−3453.

(23) Stegbauer, L.; Schwinghammer, K.; Lotsch, B. V. Postsynthetically Modified Covalent Organic Frameworks for Efficient and Effective Mercury Removal. *Chem. Sci.* **2014**, *5*, 2789–2793.

(24) Vyas, V. S.; Haase, F.; Stegbauer, L.; Savasci, G.; Podjaski, F.; Ochsenfeld, C.; Lotsch, B. V. A tunable azine covalent organic framework platform for visible light-induced hydrogen generation. *Nat. Commun.* **2015**, *6*, 8508.

(25) Guo, J.; Xu, Y.; Jin, S.; Chen, L.; Kaji, T.; Honsho, Y.; Addicoat, M. A.; Kim, J.; Saeki, A.; Ihee, H.; Seki, S.; Irle, S.; Hiramoto, M.; Gao, J.; Jiang, D. Conjugated organic framework with three-dimensionally ordered stable structure and delocalized π clouds. *Nat. Commun.* **2013**, *4*, 2736.

(26) Zhang, B.; Wei, M.; Mao, H.; Pei, X.; Alshmimri, S. A.; Reimer, J. A.; Yaghi, O. M. Crystalline Dioxin-Linked Covalent Organic Frameworks from Irreversible Reactions. *J. Am. Chem. Soc.* **2018**, *140*, 12715−12719.

(27) Guan, X.; Li, H.; Ma, Y.; Xue, M.; Fang, Q.; Yan, Y.; Valtchev, V.; Qiu, S. Chemically stable polyarylether-based covalent organic frameworks. *Nat. Chem*. **2019**, *11*, 587−594.

(28) Fang, Q.; Wang, J.; Gu, S.; Kaspar, R. B.; Zhuang, Z.; Zheng, J.; Guo, H.; Qiu, S.; Yan, Y. 3D Porous Crystalline Polyimide Covalent Organic Frameworks for Drug Delivery. *J. Am. Chem. Soc.* **2015**, *137,* 8352−8355.

(29) Lyu, H.; Diercks, C. S.; Zhu, C.; Yaghi, O. M. Porous Crystalline Olefin-Linked Covalent Organic Frameworks. *J. Am. Chem. Soc.* **2019**, *141*, 6848−6852.

(30) Xu, J.; He, Y.; Bi, S.; Wang, M.; Yang, P.; Wu, D.; Wang, J.; Zhang, F. An Olefin-Linked Covalent Organic Framework as a Flexible Thin-Film Electrode for a High-Performance Micro-Supercapacitor. *Angew. Chem. Int. Ed.* **2019**, *58*, 12065−12069.

(31) Wei, S.; Zhang, F.; Zhang, W.; Qiang, P.; Yu, K.; Fu, X.; Wu, D.; Bi, S.; Zhang, F. *Semiconducting 2D Triazine-Cored Covalent Organic Frameworks with Unsubstituted Olefin Linkages. J. Am. Chem. Soc*. **2019**, *141*, 14272−14279.

(32) Acharjya, A.; Pachfule, P.; Roeser, J.; Schmitt, F. J.; Thomas, A. Vinylene-Linked Covalent Organic Frameworks by Base-Catalyzed Aldol Condensation. *Angew Chem Int Ed*, **2019**, *58*, 14865−14870.

(33) Pyles, D. A.; Crowe, J. W.; Baldwin, L. A.; McGrier, P. L. Synthesis of Benzobisoxazole-Linked Two-Dimensional Covalent Organic Frameworks and Their Carbon Dioxide Capture Properties. *ACS Macro. Lett.* **2016**, *5*, 1055−1058.

(34) Wei, P. F.; Qi, M. Z.; Wang, Z. P.; Ding, S. Y.; Yu, W.; Liu, Q.; Wang, L. K.; Wang, H. Z. An, W. K., Wang, W. Benzoxazole-Linked Ultrastable Covalent Organic Frameworks for Photocatalysis. *J. Am. Chem. Soc*. **2018**, *140*, 4623−4631.

(35) Waller, P. J.; Al Faraj, Y. S.; Diercks, C. S.; Jarenwattananon, N. N.; Yaghi, O. M. Conversion of Imine to Oxazole and Thiazole Linkages in Covalent Organic Frameworks. *J. Am. Chem. Soc*. **2018**, *140*, 9099−9103.

(36) Shinde, D. B.; Aiyappa, H. B.; Bhadra, M.; Biswal, B. P.; Wadge, P.; Kan-dambeth, S.; Garai, B.; Kundu, T.; Kurungot, S.; Banerjee, R. A mechanochemically synthesized covalent organic framework as a proton-conducting solid electrolyte. *J. Mater. Chem. A* **2016**, *4*, 2682–2690.

(37) Heeger, A. J. Semiconducting polymers: the Third Generation. *Chem. Soc. Rev*. **2010**, *39*, 2354−2371.

(38) Li, H.; Chang, J.; Li, S.; Guan, X.; Li, D.; Li, C.; Tang, L.; Xue, M.; Yan, Y.; Valtchev, V.; Qiu, S.; Fang, Q. Three-Dimensional Tetrathiafulvalene-Based Covalent Organic Frameworks for Tunable Electrical Conductivity. *J. Am. Chem. Soc.* **2019**, *141*, 13324−13329.

(39) Medishetty, R.; Park, I. H.; Lee, S. S.; Vittal, J. J. Solid-state polymerisation via [2+2] cycloaddition reaction involving coordination polymers. *Chem. Commun*. **2016**, *52*, 3989–4001.

(40) Jon, S. Y.; Ko, Y. H.; Park, S. H.; Kim, H. H.; Kim, K. A facile, stereoselective [2 + 2] photoreaction mediated by cucurbit[8]uril. *Chem. Commun.* **2001**, 1938–1939.

(41) Lee, J. W.; Samal, S.; Selvapalam, N.; Kim, H. J.; Kim, K. Cucurbituril Homologues and Derivatives: New Opportunities in Supramolecular Chemistry. *Acc. Chem. Res.* **2003**, *36*, 621–630.

(42) Chen, Y.; Huang, F.; Li, Z.-T.; Liu, Y. *Sci. China Chem*. **2018**, *61*, 979–992.

(43) Yang, X.; Liu, F.; Zhao, Z.; Liang, F.; Zhang, H.; Liu, S. Cucurbit[10]uril-based chemistry. *Chin. Chem. Lett.* **2018**, *29*, 1560–1566.

(44) Zhang, C. C.; Zhang, Y. M.; Zhang, Z. Y.; Wu, X.; Yu, Q.; Liu, Y. Photoreaction-driven two-dimensional periodic polyrotaxane-type supramolecular nanoarchitecture. *Chem. Commun*. **2019**, *55*, 8138–8141.

(45) Tian, J.; Wang, H.; Zhang, D.-W.; Liu, Y.; Li, Z.-T. Supramolecular organic frameworks (SOFs): homogeneous regular 2D and 3D pores in water. *Natl. Sci. Rev.* **2017**, *4*, 426–436.

(46) Wu, Y.-P.; Yan, M.; Gao, Z.-Z.; Hou, J.-L.; Wang, H.; Zhang, D.-W.; Zhang, J.; Li, Z.-T. Ruthenium(II)-cored supramolecular organic framework-mediated recyclable visible light photoreduction of azides to amines and cascade formation of lactams. *Chin. Chem. Lett.* **2019**, *30*, 1383–1386.

(47) Li, X.-F.; Yu, S.-B.; Yang, B.; Tian, J.; Wang, H.; Zhang, D.-W.; Liu, Y.; Li, Z.-T. A stable metal-covalent-supramolecular organic framework hybrid: enrichment of catalysts for visible light-induced hydrogen production. *Sci. China Chem.* **2018**, *61*, 830–835.

(48) Tian, J.; Zhou, T.-Y.; Zhang, S.-C.; Aloni, S.; Altoe, M. V.; Xie, S.-H.; Wang, H.; Zhang, D.-W.; Zhao, X.; Liu, Y.; Li, Z.-T. Three-dimensional periodic supramolecular organic framework ion sponge in water and microcrystals. *Nat. Commun*. **2014**, *5*, 5574.

(49) Badjić, J. D.; Nelson, A.; Cantrill, S. J.; Turnbull, W. B.; Stoddart, J. F. Multivalency and Cooperativity in Supramolecular Chemistry. *Acc. Chem. Res.* **2005**, *38*, 723–732.

(50) Xu, J. F.; Chen, L.; Zhang, X. How to Make Weak Noncovalent Interactions Stronger. *Chem. Eur. J*. **2015**, *21*, 11938–11946.

(51) Chen. Y; Shi, Z. L.; Wei, L.; Zhou, B.; Tan, J.; Zhou, H. L.; Zhang, Y. B. Guest-Dependent Dynamics in a 3D Covalent Organic Framework. *J. Am. Chem. Soc.* **2019**, *141*, 3298−3303.

(52) Ma, Y.-X., Li, Z.-J.; Wei. L.; Ding, S.-Y.; Zhang, Y.-B.; Wang, W. A Dynamic Three-Dimensional Covalent Organic Framework. *J. Am. Chem. So*c. **2017**, *139*, 4995−4998.

(53) Geletii, Y. V.; Huang, Z.; Hou, Y.; Musaev, D. G.; Lian, T.; Hill, C. L. Homogeneous Light-Driven Water Oxidation Catalyzed by a Tetraruthenium Complex with All Inorganic Ligands. *J. Am. Chem. Soc.* **2009**, *131*, 7522–7523.

(54) Yu, S.-B.; Qi, Q.; Yang, B.; Wang, H.; Zhang, D.-W.; Liu, Y.; Li, Z.-T. Enhancing Hydrogen Generation Through Nanoconfinement of Sensitizers and Catalysts in a Homogeneous Supramolecular Organic Framework. *Small* **2018**, *14*, 1801037.

(55) Yan, M.; Liu, X.-B.; Gao, Z.-Z.; Wu, Y.-P.; Hou, J.-L.; Wang, H.; Zhang, D.-W.; Liu, Y.; Li, Z.-T. A pore-expanded supramolecular organic framework and its enrichment of

photosensitizers and catalysts for visible-light-induced hydrogen production. *Org. Chem. Front.* **2019**, *6*, 1698–1704.

TOC graphic